Computer simulation study of a simple cubatic mesogenic lattice model

Silvano Romano*
Unità di Ricerca CNISM e Dipartimento di Fisica "A. Volta," Università di Pavia, via A. Bassi 6, I-27100 Pavia, Italy
(Received 16 March 2006; published 11 July 2006)

Over the last 15 years, the possible existence of a cubatic mesophase, possessing cubic orientational order (i.e., along three mutually orthogonal axes) but no translational one, has been addressed theoretically, and predicted in some cases, where the investigated interaction models involved hard-core repulsion only; on the other hand, no experimental realizations of such a phase are known at the time being. The present paper addresses a very simple cubatic mesogenic lattice model, involving continuous interactions; we consider particles possessing O_h symmetry, whose centers of mass are associated with a three-dimensional simple-cubic lattice; the pair potential is taken to be isotropic in orientation space, and restricted to nearest neighboring sites; let the two orthonormal triads $\{\mathbf{u}_j,\ j=1,2,3\}$ and $\{\mathbf{v}_k,\ k=1,2,3\}$ define orientations of a pair of interacting particles, and let $f_{jk}=\mathbf{v}_j\cdot\mathbf{u}_k$. The interaction model studied here is defined by the simplest nontrivial (quartic) polynomial in the scalar products f_{jk}, consistent with the assumed symmetry and favoring orientational order; it is, so to speak, the cubatic counterpart of the Lebwohl-Lasher model for uniaxial nematics. The model was investigated by mean field theory and Monte Carlo simulation, and found to produce a low-temperature cubatically ordered phase, undergoing a first order transition to the isotropic phase at higher temperature; the mean field treatment yielded results in reasonable qualitative agreement with simulation.

DOI: 10.1103/PhysRevE.74.011704 PACS number(s): 61.30.−v, 61.30.Cz, 61.30.Gd, 64.70.Md

INTRODUCTION AND POTENTIAL MODELS

Over the last three decades, theoretical studies of various simple mesogenic models have predicted a rather rich and intriguing phase behavior, whose experimental realization has often proven to be a rather challenging task of its own. For example, the possible existence of biaxial nematic phases was predicted by various theoretical treatments since 1970 [1], and is still currently investigated. On the experimental side, stable biaxial phases have been observed in lyotropic systems as early as 1980 [2]; since 1986 there have been various claims and counterclaims of synthesizing and unambiguosly characterizing a thermotropic biaxial nematic and better experimental evidence seems to have been produced over the last two years; a more detailed discussion and a more extensive bibliography can be found in Ref. [3].

As another example, over the last 15 years, the possible existence of a cubatic mesophase, possessing cubic orientational order (i.e., along three mutually orthogonal axes) but no translational one, has been investigated theoretically, and explicitly predicted in some cases [4–9]): cut hard spheres were studied in Refs. [4,5]; the possible existence of cubatic order for hard cylinders was investigated in Ref. [6], but no evidence of it was found in this case; Onsager crosses were studied in Ref. [7]; arrays of hard spheres with tetragonal or cubic symmetry have been studied in Refs. [8,9]. The named investigations have been carried out on hard-core models, both by simulation and by approximate analytical theories; in some cases the consituent particles were uniaxial (i.e., $D_{\infty h}$ symmetric) [4–6], and in other cases they possessed tetragonal or cubic symmetry [7–9]. As hinted above, no experimental realizations of a cubatic phase are known at the time being.

On the other hand, over the decades, mesophases possessing no positional order, such as the nematic one, have often and quite fruitfully been studied by means of lattice models involving continuous interaction potentials [10], starting with the Lebwohl-Lasher (LL) model and its seminal simulation papers in the early 1970s [11,12]; this approach also yields a convenient contact with molecular field (MF) treatments of the Maier-Saupe (MS) type [13–15].

Here we investigate a very simple lattice model capable of producing cubatic order: we are considering classical, identical particles, possessing O_h symmetry, whose centers of mass are associated with a three-dimensional (simple-cubic) lattice $\mathbb{Z}^3$; let $\mathbf{x}_\mu\in\mathbb{Z}^3$ denote the coordinate vectors of their centers of mass; the interaction potential is taken to be isotropic in orientation space, and restricted to nearest neighbors, involving particles or sites labeled by μ and ν, respectively. The orientation of each particle can be specified via an orthonormal triplet of three-component vectors (e.g., eigenvectors of its inertia tensor), say $\{\mathbf{w}_{\mu,j},\ j=1,2,3\}$; in turn these are controlled by an ordered triplet of Euler angles $\Omega_\mu=\{\phi_\mu,\theta_\mu,\psi_\mu\}$; particle orientations are defined with respect to a common, but otherwise arbitrary, Cartesian frame (which can, but need not, be identified with the lattice frame). It also proves convenient to use a simpler notation for the unit vectors defining orientations of two interacting molecules [16], i.e., $\mathbf{u}_j$ for $\mathbf{w}_{\mu,j}$, and $\mathbf{v}_k$ for $\mathbf{w}_{\nu,k}$, respectively, here, for each j, $\mathbf{u}_j$ and $\mathbf{v}_j$ have the same functional dependences on Ω_μ and Ω_ν, respectively (pairs of corresponding unit vectors in the two interacting molecules); let $\tilde{\Omega}=\Omega_{\mu\nu}=\{\tilde{\phi},\tilde{\theta},\tilde{\psi}\}$ denote the set of Euler angles defining the rotation transforming $\mathbf{u}_j$ into $\mathbf{v}_j$; Euler angles will be defined here according to the convention used by Brink and Satchler [17–19]; let us finally define

$$f_{jk}=(\mathrm{v}_j\cdot\mathrm{u}_k). \tag{1}$$

An interaction potential consistent with the assumed symmetry can be written

*Electronic address: silvano.romano@pv.infn.it

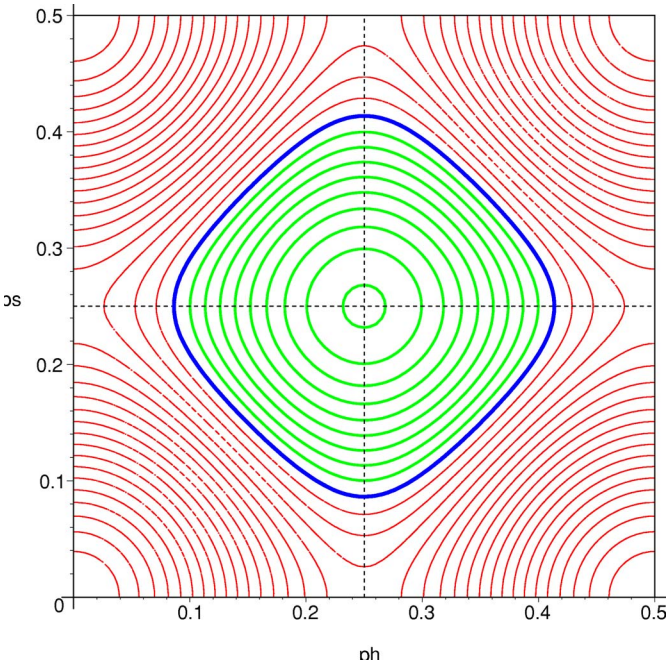

FIG. 1. (Color online) Contour plot for the function $H(\pi/2)$ [see Eq. (7)]; the contour-to-contour separation is 0.05ϵ; thin (red) lines correspond to negative values, thicker (green) lines are associated with positive values, and the thickest (blue) one defines the zero-energy contour. The plot was produced by means of Maple.

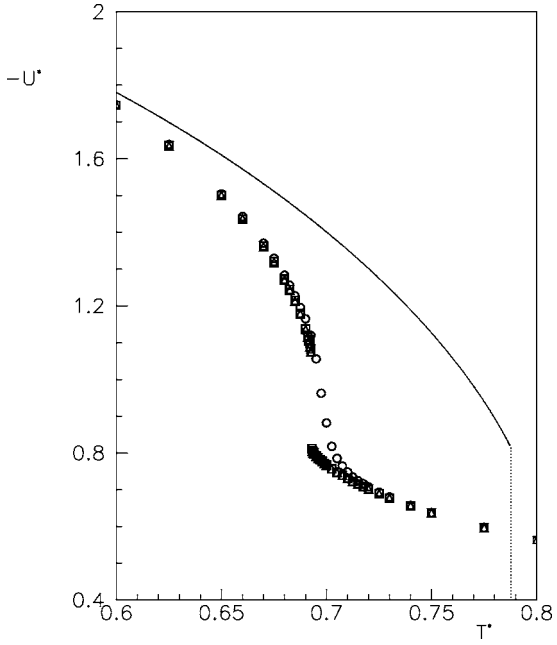

FIG. 2. MF predictions and simulation results for the potential energy; the continuous line corresponds to MF predictions, discrete symbols have been used for simulation results, obtained with different sample sizes, and have the following meanings: circles, $q=10$; squares, $q=20$; triangles, $q=30$; unless otherwise stated or shown, here and in the following figures, the associated statistical errors fall within symbol sizes.

$$\Psi = \Psi_{\mu\nu} = \sum_{j=1}^{3}\sum_{k=1}^{3} E(f_{jk}), \tag{2}$$

here $E(\cdots)$ denotes an even function of its argument; E is also assumed to be analytical, so that Eq. (2) can be expanded as a convergent series of the form

$$\Psi = a_0 + \sum_{l\geqslant 2} a_{2l}\left(\sum_{j=1}^{3}\sum_{k=1}^{3}(f_{jk})^{2l}\right) = b_0 + \sum_{l\geqslant 2} b_{2l}\left(\sum_{j=1}^{3}\sum_{k=1}^{3} P_{2l}(f_{jk})\right), \tag{3}$$

where $P_{2l}(\cdots)$ denotes Legendre polynomials of even order, and the missing second-order terms are just constants, i.e.,

$$\sum_{j=1}^{3}\sum_{k=1}^{3} f_{jk}^2 = 3, \quad \sum_{j=1}^{3}\sum_{k=1}^{3} P_2(f_{jk}) = 0. \tag{4}$$

The simplest interaction model expected to produce cubatic order is obtained by setting a_4 or b_4 to negative quantities, and all other higher-order coefficients to zero; in other words

$$\Psi = -\frac{1}{6}\epsilon\left(5\sum_{j=1}^{3}\sum_{k=1}^{3}(f_{jk}^4) - 9\right) = -\frac{4}{21}\epsilon\sum_{j=1}^{3}\sum_{k=1}^{3} P_4(f_{jk}) = -\epsilon G_4(\tilde{\Omega}), \tag{5}$$

where ϵ denotes a positive quantity, setting energy and temperature scales (i.e., $T^* = k_B T/\epsilon$); here numerical factors have been adjusted by setting the isotropic average of the pair potential to zero (i.e., $b_0=0$), and its minimum value to $-\epsilon$. The explicit expression of $G_4(\tilde{\Omega})$ reads

$$\begin{aligned} G_4(\tilde{\Omega}) &= \tfrac{1}{12}\{7\Delta_{0,0}^4(\tilde{\Omega}) + \sqrt{35}[\Delta_{0,4}^4(\tilde{\Omega}) + \Delta_{4,0}^4(\tilde{\Omega})] + 5\Delta_{4,4}^4(\tilde{\Omega})\} \\ &= \tfrac{1}{768}(140\cos(2\tilde{\theta})[1+\cos(4\tilde{\phi})\cos(4\tilde{\psi})] \\ &\quad + 5\cos(4\tilde{\theta})[49+\cos(4\tilde{\phi})\cos(4\tilde{\psi})] \\ &\quad + 7\{9 + 25\cos(4\tilde{\phi})\cos(4\tilde{\psi}) + 40[\cos(4\tilde{\phi}) \\ &\quad + \cos(4\tilde{\psi})](\sin\tilde{\theta})^4\} - 40[7\cos(\tilde{\theta}) \\ &\quad + \cos(3\tilde{\theta})]\sin(4\tilde{\phi})\sin(4\tilde{\psi})). \end{aligned} \tag{6}$$

The functions $\Delta_{p,q}^4$ appearing in Eq. (6) are symmetry-adapted combinations of Wigner $\mathcal{D}$ functions, as discussed in Refs. [7,20,21].

$G_4(\tilde{\Omega})$ is a function of three independent variables, and in practice its visualization requires using projections (i.e., constraining one of the three independent variables); for example, let α denote a fixed angle, and let

$$H(\alpha) = -\epsilon G_4(\tilde{\phi}, \tilde{\theta} = \alpha, \tilde{\psi}); \tag{7}$$

contour plots for $H(\pi/2)$ are shown in Fig. 1.

MEAN FIELD AND SIMULATION ASPECTS

After applying a MF procedure [15], the resulting expression for the free energy has the form

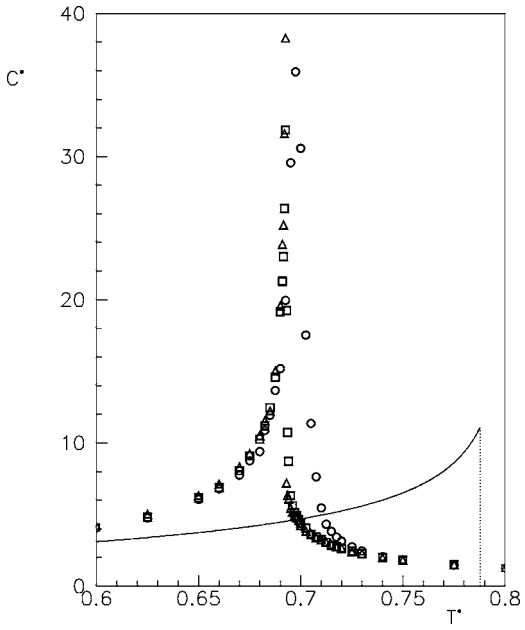

FIG. 3. MF predictions and simulation results for the configurational heat capacity; same meaning of symbols as in Fig. 2; here the associated statistical errors, not shown, range between 1% and 5%.

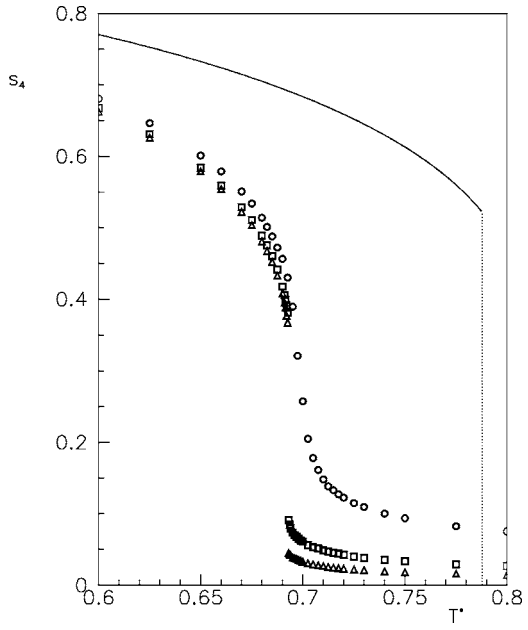

FIG. 4. MF predictions and simulation results for the order parameters s_4, obtained with different sample sizes; same meaning of symbols as in Fig. 2.

$$A^*_{\mathrm{MF}} = \rho s_4^2 - T^* \ln[\Xi/(8\pi^2)], \quad \Xi = \int_{\mathrm{Eul}} \exp(\beta \tilde{W}) d\omega, \tag{8}$$

$$\tilde{W} = 2\rho s_4 G_4(\omega), \quad \beta = 1/T^*, \tag{9}$$

where $\int_{\mathrm{Eul}}$ denotes integration over Euler angles, i.e., for any integrable function $\mathcal{F}(\omega)$

$$\int_{\mathrm{Eul}} \mathcal{F}(\omega) d\omega \equiv \int_0^{2\pi} d\phi \int_0^{\pi} \sin\theta d\theta \int_0^{2\pi} \mathcal{F}(\omega) d\psi; \tag{10}$$

here $2\rho=6$ denotes the lattice coordination number, and s_4 is the variational parameter (i.e., the order parameter). Moreover

$$\frac{\partial A^*_{\mathrm{MF}}}{\partial s_4} = (2\rho)\tau; \quad \tau = s_4 - (1/\Xi) \int_{\mathrm{Eul}} G_4(\omega) \exp(\beta \tilde{W}) d\omega, \tag{11}$$

and the consistency equation is $\tau=0$.

The free energy was minimized numerically for each temperature over a fine grid, by means of numerical routines using both the function [Eq. (8)] and its derivative [Eq. (11)]; the obtained variational parameters were used to calculate the potential energy per particle U^*_{MF}

$$U^*_{\mathrm{MF}} = \frac{\partial(\beta A^*_{\mathrm{MF}})}{\partial \beta} = -\rho s_4^2, \tag{12}$$

where the consistency equation has been allowed for on the right-hand expression; the configurational specific heat C^*_{MF} was then calculated from U^*_{MF} by numerical differentiation; here and in the following formulas, asterisks mean scaling by ϵ for energy quantities, and scaling by k_B for the specific heat. We found a low-temperature ordered phase and a first-order transition to the disordered one, taking place at the temperature $\Theta_{\mathrm{MF}}=0.7878$.

Simulations were carried out on a periodically repeated cubic sample, consisting of $V=q^3$ particles, $q=10,20,30$; calculations were run in cascade, in order of increasing temperature, and starting from a perfectly ordered configuration at the lowest investigated temperature; each cycle (or sweep) consisted of $2V$ MC steps, including a sublattice sweep [22]; the finest temperature step used was $\Delta T^*=0.0005$, in the transition region.

Notice that we shall find here a pronounced first-order transition, and that simulations carried out in order of decreasing temperature and started from the disordered high-temperature régime may show hysteresis.

Different random-number generators were used, as discussed in Ref. [22]. Equilibration runs took between 25 000 and 100 000 cycles, and production runs took between 200 000 and 800 000; macrostep averages for evaluating statistical errors were taken over 1000 cycles. Calculated thermodynamic quantities include mean potential energy per site U^* and configurational specific heat per particle C^*.

As for the the frame-independent (rotationally invariant) order parameter, let

$$M = \sqrt{\left(\frac{4}{21}\right) \sum_{\lambda=1}^{V} \sum_{\nu=1}^{V} \left(\sum_{j=1}^{3} \sum_{k=1}^{3} P_4(\mathbf{w}_{\lambda,j} \cdot \mathbf{w}_{\mu,k}) \right)}; \tag{13}$$

then the simulation estimate for the order parameter is

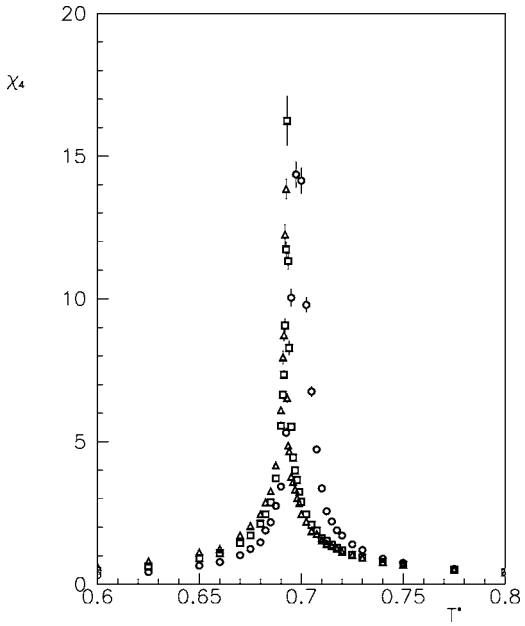

FIG. 5. Simulation results for the order parameter susceptibility χ_4, obtained with different sample sizes: same meaning of symbols as in Fig. 2.

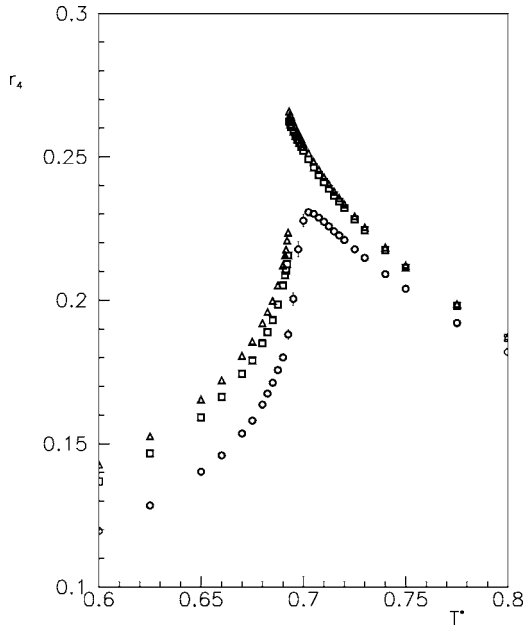

FIG. 6. Simulation results for the correlation excess r_4 [see Eq. (18)], obtained with different sample sizes: same meaning of symbols as in Fig. 2.

$$s_4 = \frac{1}{V}\langle M \rangle, \tag{14}$$

and its associated susceptibility reads

$$\chi_4 = \frac{1}{V}\beta(\langle M^2 \rangle - \langle M \rangle^2). \tag{15}$$

As for computational aspects of Eq. (13), let us remark that, by the addition theorem for spherical harmonics [17–19], the double sums appearing in it can be constructed via single sums [7], i.e., as linear combinations of the squares of the simpler quantities

$$\xi_{j,m} = \sum_{\mu=1}^{V} \mathrm{Re}[C_{4,m}(\mathbf{w}_{\mu,j})], \quad \eta_{j,m} = \sum_{\mu=1}^{V} \mathrm{Im}[C_{4,m}(\mathbf{w}_{\mu,j})]; \tag{16}$$

here $m=0,1,2,3,4$, $C_{4,m}(\cdots)$ are modified spherical harmonics, and Re and Im denote real and imaginary parts, respectively; in turn, each spherical harmonics is a suitable polynomial constructed in terms of Cartesian components of the corresponding unit vector (see, e.g., Ref. [23]); notice also that in this case all second-rank order parameters are zero by symmetry [15].

One can also evaluate the so-called short-range order parameter [24,25]

$$\sigma_4 = \frac{4}{21}\left\langle \sum_{j=1}^{3}\sum_{k=1}^{3} P_4(f_{jk}) \right\rangle \tag{17}$$

measuring correlations between pairs molecules associated with nearest-neighboring sites; in the present case, the functional form of the interaction potential entails that the potential energy is proportional to σ_4, i.e., $U^* = -\rho\sigma_4$.

Long- and short-range orientational order can be compared via the correlation excess

$$r_4 = \sigma_4 - s_4^2. \tag{18}$$

RESULTS AND COMPARISONS

MF predictions and MC results for a few observables are plotted and compared in Figs. 2–6.

Simulation results for the potential energy (Fig. 2) are independent of sample size for $T \lesssim 0.68$ and then $T \gtrsim 0.72$, and show a pronounced sample-size dependence in between; actually, already for $q=20$, Figure 2 exhibts a pronounced jump taking place over a temperature range of 0.0005.

Figure 4 shows a similar pattern as for the jump of s_4, taking place at the same temperature as for U^*; on the other hand, in the low-temperature regime, sample-size effects appear to saturate for $q \geqslant 20$, and the high-temperature region exhibits a pronounced decrease of s_4 with increasing sample size.

Both configurational specific heat (Fig. 3) and susceptibility (Fig. 5) peak around the same temperature, corresponding to the named jumps; they show a recognizable sample-size dependence over the same temperature range $0.68 \lesssim T^*$

TABLE I. Transitional properties for the investigated model; MC results are based on the largest investigated sample size $q=30$.

Method	Θ	ΔU^*	s_4
MF	0.7878	0.8181	0.5222
MC	0.692±0.001	0.28±0.04	0.38±0.02

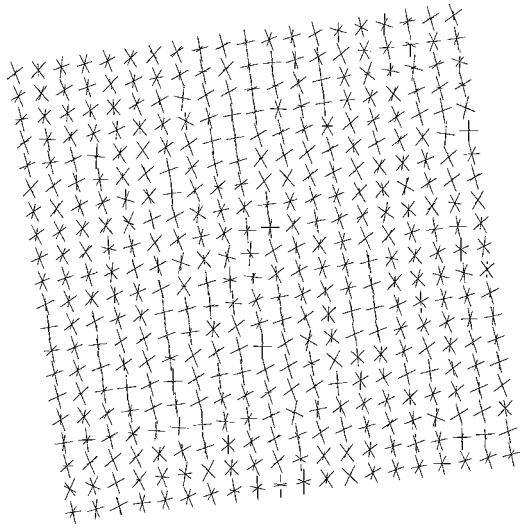

FIG. 7. Partial configuration obtained by simulation at $T^*=0.675$, and from a sample with $q=20$; see also the text.

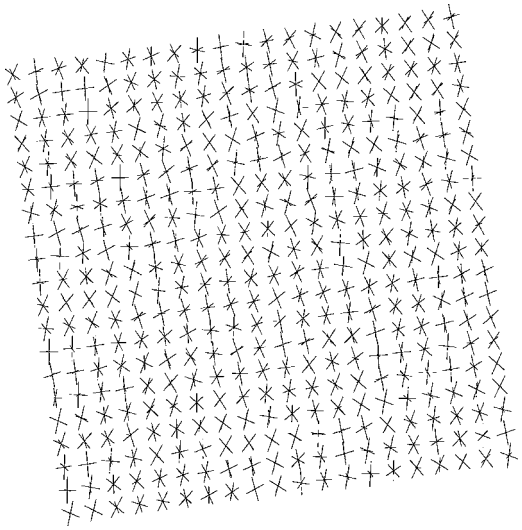

FIG. 8. Partial configuration obtained by simulation at $T^*=0.700$, and from a sample with $q=20$.

$\lesssim 0.72$, and are again largely unaffected by sample sizes outside it.

Simulation results for the correlation excess are plotted in Fig. 6, where the transition is signaled by both a peak and a recognizable jump; in the disordered region, sample-size effects appear to saturate for $q \geqslant 20$.

Thus we propose a first-order transition, and the value $\Theta_{MC}=0.692\pm0.001$, for the transition temperature; here the error bar is conservatively taken to be twice the temperature step used in the transition region. Upon analyzing the simulation results for the largest sample as discussed in Refs. [26,27], we obtained the estimates for transitional properties collected in Table I; actually, the same analysis was also applied to simulation results obtained for $q=20$, and yielded consistent results. Table I shows a fair qualitative agreement between MF and MC; of course, in quantitative terms MF overestimates the transition temperature, and, even worse, its first-order character, as well known for LL; let us mention, for comparison, that the ratio Θ_{MC}/Θ_{MF} is ≈ 0.878, and that the corresponding value for LL is ≈ 0.856 [10].

Partial snapshots of configurations extracted from a sample defined by $q=20$ and obtained at temperatures below and above the transition ($T^*=0.675$ and $T^*=0.7$) are shown in Figs. 7 and 8, respectively. More precisely, in order to maintain readability, we decided to show only a horizontal section of the sample, i.e., the square layer consisting of (q^2) particles whose centers of mass had the same value for the vertical z coordinate; the arbitrarily chosen value was $q/2$. To summarize, we have defined a very simple cubatic mesogenic lattice model (so to speak, the cubatic counterpart of LL), involving continuous interactions, and investigated it by MF and MC; both approaches show a first-order transition, and MF produces a reasonable qualitative agreement with MC.

ACKNOWLEDGMENTS

The present extensive calculations were carried out, on, among other machines, workstations belonging to the Sezione di Pavia of Istituto Nazionale di Fisica Nucleare (INFN); allocations of computer time by the Computer Centre of Pavia University and CILEA (Consorzio Interuniversitario Lombardo per l' Elaborazione Automatica, Segrate-Milan), as well as by CINECA (Centro Interuniversitario Nord-Est di Calcolo Automatico, Casalecchio di Reno-Bologna), are gratefully acknowledged. The author also wishes to thank Professor L. Longa (Krakow, Poland), Professor G. R. Luckhurst (Southampton, England, UK), Professor E. G. Virga (Pavia, Italy), and Dr. R. Blaak (Cambridge, England, UK) for helpful discussions and suggestions. Finally, the author gratefully acknowledges financial support from the Italian Ministry for Higher Education (MIUR) through the PRIN Grant No. 2004024508.

[1] M. J. Freiser, Phys. Rev. Lett. **24**, 1041 (1970).
[2] L. J. Yu and A. Saupe, Phys. Rev. Lett. **45**, 1000 (1980).
[3] G. R. Luckhurst, Angew. Chem., Int. Ed. **44**, 2836 (2005).
[4] J. A. C. Veerman and D. Frenkel, Phys. Rev. A **45**, 5632 (1992).
[5] A. Chamoux and A. Pereira, J. Chem. Phys. **108**, 8172 (1998).
[6] R. Blaak, D. Frenkel, and B. M. Mulder, J. Chem. Phys. **110**, 11652 (1999).
[7] R. Blaak and B. M. Mulder, Phys. Rev. E **58**, 5873 (1998).
[8] B. S. John, A. Stroock, and F. A. Escobedo, J. Chem. Phys. **120**, 9383 (2004).
[9] B. S. John, A. Stroock, and F. A. Escobedo, J. Phys. Chem. B **109**, 23008 (2005).
[10] P. Pasini, C. Chiccoli, and C. Zannoni, *Advances in the Com-*

puter Simulations of Liquid Crystals, edited by P. Pasini and C. Zannoni, NATO Science Series C: Mathematical and Physical Sciences, Vol. 545 (Kluwer, Dordrecht, 2000), Chap. 5.
[11] P. A. Lebwohl and G. Lasher, Phys. Rev. A **5**, 1350 (1972).
[12] G. Lasher, Phys. Rev. A **6**, 426 (1972).
[13] W. Maier and A. Saupe, Z. Naturforsch. A **13A**, 564 (1958); **14A**, 882 (1959); **15**, 287 (1960).
[14] G. R. Luckhurst, in *The Molecular Physics of Liquid Crystals*, edited by G. R. Luckhurst and G. W. Gray (Academic, London, 1979), Chap. 4, pp. 85–120.
[15] G. R. Luckhurst, in *Physical Properties of Liquid Crystals: Nematics*, edited by D. A. Dunmur, A. Fukuda, and G. R. Luckhurst (INSPEC, London, UK, 2001), Chap. 2.1.
[16] C. Chiccoli, P. Pasini, F. Semeria, and C. Zannoni, Int. J. Mod. Phys. C **10**, 469 (1999).
[17] D. M. Brink and G. R. Satchler, *Angular Momentum*, 2nd ed. (Oxford University Press, Oxford, UK, 1968).
[18] D. A. Varshalovich, A. N. Moskalev, and V. K. Khersonskii, *Quantum Theory of Angular Momentum* (World Scientific, Singapore, 1988).
[19] G. B. Arfken and H. J. Weber, *Mathematical Methods for Physicists*, 4th ed. (Academic, San Diego, 1995).
[20] B. M. Mulder, Liq. Cryst. **1**, 539 (1986).
[21] B. Mulder, Phys. Rev. A **39**, 360 (1989).
[22] R. Hashim and S. Romano, Int. J. Mod. Phys. B **13**, 3879 (1999).
[23] J. W. Leech and D. J. Newman, *How to Use Groups* (Methuen, London, 1969).
[24] C. Zannoni, in *The Molecular Physics of Liquid Crystals*, edited by G. R. Luckhurst and G. W. Gray (Academic, London, 1979), Chaps. 3 and 9.
[25] C. Zannoni, *Advances in the Computer Simulations of Liquid Crystals*, edited by P. Pasini and C. Zannoni, NATO Science Series C: Mathematical and Physical Sciences, Vol. 545 (Kluwer, Dordrecht, 2000), Chap. 2.
[26] S. Romano, Int. J. Mod. Phys. B **16**, 2901 (2002).
[27] S. Romano, Physica A **324**, 606 (2003).